ISSN 1063-7842, Technical Physics, 2011, Vol. 56, No. 10, pp. 1501–1507. © Pleiades Publishing, Ltd., 2011.
Original Russian Text © V.V. Balashev, V.V. Korobtsov, T.A. Pisarenko, L.A. Chebotkevich, 2011, published in Zhurnal Tekhnicheskoĭ Fiziki, 2011, Vol. 81, No. 10, pp. 122–128.

SURFACE, ELECTRON AND ION EMISSION

Growth of Fe_3O_4 Films on the Si(111) Surface Covered by a Thin SiO_2 Layer

V. V. Balashev*[a, b], V. V. Korobtsov[a, b], T. A. Pisarenko[a, b], and L. A. Chebotkevich[b]

[a] *Institute for Automation and Control Processes, Far East Branch, Russian Academy of Sciences, ul. Radio 5, Vladivostok, 690041 Russia*

[b] *Institute of Physics and Information Technologies, Far East State University, ul. Sukhanova 8, Vladivostok, 690950 Russia*

**e-mail: balashev@mail.dvo.ru*

Received January 11, 2011

Abstract—Magnetite polycrystalline films are grown by variously oxidizing a Fe film on the Si(111) surface covered by a thin (1.5 nm) SiO_2 layer. It is found that defects in the SiO_2 layer influence silicidation under heating of the Fe film. The high-temperature oxidation of the Fe film results in the formation of both Fe_3O_4 and iron monosilicide. However, the high-temperature deposition of Fe in an oxygen atmosphere leads to the growth of a compositionally uniform Fe_3O_4 film on the SiO_2 surface. It is found that such a synthesis method causes [311] texture to arise in the magnetite film, with the texture axis normal to the surface. The influence of the synthesis method on the magnetic properties of grown Fe_3O_4 films is studied. A high coercive force of Fe_3O_3 films grown by Fe film oxidation is related to their specific morphology and compositional nonuniformity.

DOI: 10.1134/S1063784211100033

INTRODUCTION

Magnetite, owing to the complete spin polarization of electrons [1] and a high Curie temperature (~580°C), is viewed as a promising material for spintronics—a new field of semiconductor electronics. Fe_3O_4 formation on the silicon surface is of interest in relation to effective injection of spin-polarized electrons from the Fe_3O_4 film to the Si substrate. A number of recent works have been devoted to the growth of magnetite films on the pure silicon surface [2, 3] and on the silicon surface covered by a buffer layer [4]. It has been found that Fe_3O_4 films grow polycrystalline irrespective of the growth technique. It was also reported that a layer including both iron silicide and amorphous iron oxide (Fe_xO_y) forms at the early stage of Fe_3O_4 growth on a Si substrate [5, 6]. This layer with a thickness of ~7 nm prevents effective injection of spin-polarized electrons from the Fe_3O_4 film to the semiconductor. A thin SiO_2 layer used as a buffer layer is necessary to prevent the formation of iron silicide. Moreover, the possibility of spin-polarized electrons injecting from the magnetite layer into an inverse layer at the interface between the Si substrate and a thin layer of natural SiO_2 layer was demonstrated [7]. Studies of the magnetite film sheet conductivity showed that an additional conductivity channel through the inverse layer along the SiO_2/Si interface arises at temperatures above 250 K. For further investigations into such effects as spin-polarized electron tunneling and current channel switchover, it is of interest to gain insight into the formation conditions of the $Fe_3O_4/SiO_2/Si$ structure. Central to the growth of this structure are the thickness and quality of the SiO_2 layer, on the one hand, and the sharpness of the interface between the Fe_3O_4 film and the SiO_2/Si structure surface, on the other.

From the available experimental data, it is known that thin Fe_3O_4 films on the semiconductor surface can be formed both by oxidation of a thin Fe layer in an oxygen atmosphere [8] and by Fe sputtering in an oxygen atmosphere [5, 9]. In this work, we report experimental data for Fe_3O_4 films grown on the SiO_2/Si(111) surface by different methods. Then thin SiO_2 overlayer was obtained by wet chemical treatment of the Si(111) surface. Also, we studied the magnetic properties of variously synthesized $Fe_3O_4/SiO_2/Si$ structures.

1. EXPERIMENT

Experiments were conducted with a Katun' ultrahigh-vacuum setup equipped with systems for reflection high-energy electron diffraction (RHEED) and spectral ellipsometry. The background pressure was no higher than 10^{-10} Torr. 0.5 × 10 × 20-mm plates cut from *p*-Si(111) wafers with a resistivity of 4.5 Ω cm were used as substrates. Prior to the substrates were loaded in the vacuum chamber, their surface was cleaned by wet chemical processing [10]. At the final stage of Si substrate surface cleaning, thin SiO_2 layers were formed by boiling in concentrated nitric acid

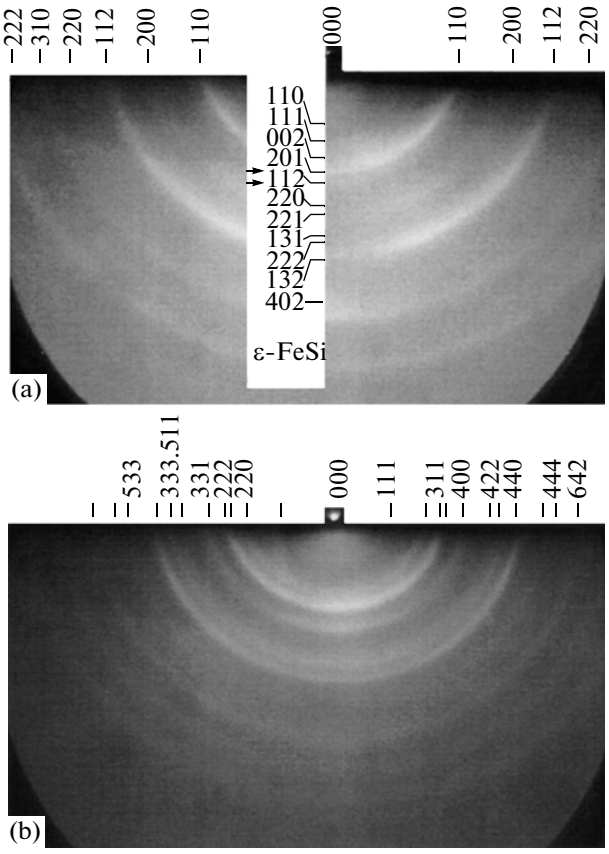

Fig. 1. RHEED pattern taken from the surface of the SiO_2/Si structure after (a) the room-temperature deposition of a Fe layer and annealing at 300°C and (b) exposure of the film to the oxygen atmosphere at a substrate temperature of 300°C. Vertical bars in both panels show the theoretical positions of Debye rings for diffraction by iron and magnetite polycrystals. A double arrow in panel "a" points to the most intense rings in the case of diffraction by ε-FeSi polycrystals.

(HNO_3) for 5 min. The SiO_2 thickness measured by spectral ellipsometry was found to be ~1.5 nm. After the substrates were loaded into the vacuum chamber, they were preheated at 500°C for 1 h. Iron was deposited on the surface of the SiO_2/Si(111) structure by thermal evaporation from a Knudsen cell with an Al_2O_3 crucible. The Fe deposition rate determined by the method suggested in [11] was 0.8 nm/min.

Magnetite films were obtained by three methods: (i) by annealing Fe films predeposited at room temperature at 300°C in an oxygen atmosphere, (ii) by heating Fe films deposited at room temperature to 300°C in an oxygen atmosphere and subsequently keeping at this temperature, and (iii) by depositing Fe films in an oxygen atmosphere at 300°C. In all the cases, the oxygen pressure in the vacuum pressure is maintained at $\sim 1.3 \times 10^{-6}$ Torr and the thickness of the iron films was 8 nm. The oxidation of such amount of iron is expected to result in the formation of a Fe_3O_4 film ~16 nm in thickness.

Information on the structural and phase compositions of the iron oxide films at different growth stages was derived from RHEED patterns. When taking RHEED patterns, the electron beam was incident to the surface at a grazing angle, ~1°. After the samples were removed from the vacuum chamber, the morphology and composition of the films were examined by atomic force microscopy (AFM) and Raman spectroscopy, respectively. Raman spectra with a resolution of 1.5 cm^{-1} were recorded with a NTEGRA Spectra probe nanolaboratory. A 488-nm laser was used as a source of Raman radiation excitation. The laser beam was focused on the sample into a spot ~0.5 μm in diameter. The laser radiation power on the sample surface was equal to 8 mW. The magnetic properties of the films were studied using a vibrating sample magnetometer.

2. RESULTS AND DISCUSSION

After Fe films were deposited on the surface of the SiO_2/Si(111) structure at room temperature, the RHEED patterns exhibited diffuse rings with a nonuniform intensity distribution, which is typical of transmission diffraction from a textured polycrystalline film. These rings indicate the presence of [110] texture, which is typical of Fe films grown on the SiO_2 surface at room temperature [12]. Then, the Fe film was oxidized by heating to 300°C at a rate of 15°C/min in the oxygen atmosphere. Figure 1a shows the RHEED pattern taken of the surface after the heating. During heating of the substrate, the rings from the Fe film (vertical bars in Fig. 1a) become sharper, suggesting coarsening of the crystallites. In addition, the postheating distribution of the Fe ring intensity becomes more uniform, because the preferred orientation of Fe crystallites disappears. Along with Fe ring sharpening in the RHEED pattern, extra faint rings arise. The positions of these rings (horizontal bars in Fig. 1a) correlate with the inverse values of the interplanar distances ($1/d_{hkl}$) in ε-FeSi iron monosilicide with a cubic structure (structure B20). The RHEED pattern shows that the most intense rings from this group are the (201) and (112) reflections (arrows in Fig. 1a). A high intensity of these reflections was also observed in [13], where polycrystalline ε-FeSi iron monosilicide films grown on the pure silicon surface were studied. The rise in the intensity of the diffraction ring corresponding to an interplanar distance of ~0.2 nm is explained by the superposition of the (201) diffraction ring from ε-FeSi and (110) ring from Fe (the respective interplanar distances coincide). The observed diffraction pattern remained unchanged for 10 min of heating–exposure at 300°C.

Subsequent annealing of the Fe film in the oxygen atmosphere for 10 min causes Fe rings in the RHEED pattern to disappear and new diffraction rings to arise (Fig. 1b). The positions of the new rings agree with theoretical positions (vertical bars) calculated for a

magnetite lattice with an inverse spinel structure [14]. The time taken of the RHEED pattern to change to the new one is about 1 min after the onset of exposure at an oxygen pressure of about 1.3×10^{-6} Torr in the vacuum chamber. The intensity of magnetite rings increased with time of exposure. Upon the oxidation of the Fe film, rings from ε-FeSi are absent in the RHEED pattern. A possible reason for this effect may be enhanced scattering of electrons incident on the surface at a grazing angle by Fe_3O_4 crystallites, which grow in size twofold upon oxidation compared with Fe crystallites.

The AFM image taken of the surface of this film (Fig. 2) shows that most crystallites in it are about 50 nm across (crystallites *A*). Coarser crystallites (more than 100 nm across) are also present on the surface (crystallites *B*). The density of the latter, $\sim 3 \times 10^8$ cm^{-2}, is twice as low as that of the former. Their formation may be associated with the formation both of ε-FeSi as a result of heating the Fe film and of another phase of iron oxide. It is known that the structure of maghemite (γ-Fe_2O_3) is the same as that of magnetite and the lattice constant of the former (0.8342 nm) is almost the same as that of the latter, 0.8396 nm. Since the positions of diffraction rings for these oxides will nearly coincide, identification of maghemite by RHEED seems to be problematic. To identify the structure of these films, we conducted Raman studies. The inset to Fig. 2 shows the Raman spectrum taken of the iron oxide film. It was found that the oxidation of iron gives rise to one more peak at ~670 cm^{-1} in addition to peaks from the silicon substrate at ~303, 619, and 520 cm^{-1}. According to theoretical calculations [15], there are five active Raman modes in crystalline magnetite at room temperature: mode A_{1g} ($\omega = 669$ cm^{-1}), mode E_g ($\omega = 410$ cm^{-1}), and three T_{2g} modes [$\omega(T_{2g}^1 = 193\,\text{cm}^{-1})$, $\omega(T_{2g}^2 = 540\,\text{cm}^{-1})$, and $\omega(T_{2g}^3 = 300\,\text{cm}^{-1})$]. Since the Raman spectrum from magnetite typically contains intense peaks at 669 and 540 cm^{-1}, the peak at ~670 cm^{-1} present in the spectrum can be related to magnetite. The magnetite peak at 540 cm^{-1} is invisible, since it is weak and superposes on the silicon peak at 520 cm^{-1}.

In [16], heating of a Fe film grown on the oxidized Si surface resulted in silicidation at defects in the SiO_2 layer because of interdiffusion between Fe and Si atoms. Eventually, iron silicide islands formed, the density of which (~10^8 cm^{-2}) was comparable to the density of defects in the SiO_2 film. With the experimental data of this work taken into account, we suppose that large islands observed in the AFM image are iron monosilicide crystallites at defects in the SiO_2 layer. This supposition is confirmed both by the appearance of diffraction rings from ε-FeSi upon heating the Fe film (Fig. 1a) and by the density of these islands (3×10^8 cm^{-2}), which is comparable to the above value. Because of the low density of ε-FeSi islands on the surface, the intensity of rings due to diffraction by ε-FeSi crystallites is low and the intense peak at ~315 cm^{-1} (*E* mode) corresponding to this iron silicide [17] is absent in the Raman spectrum.

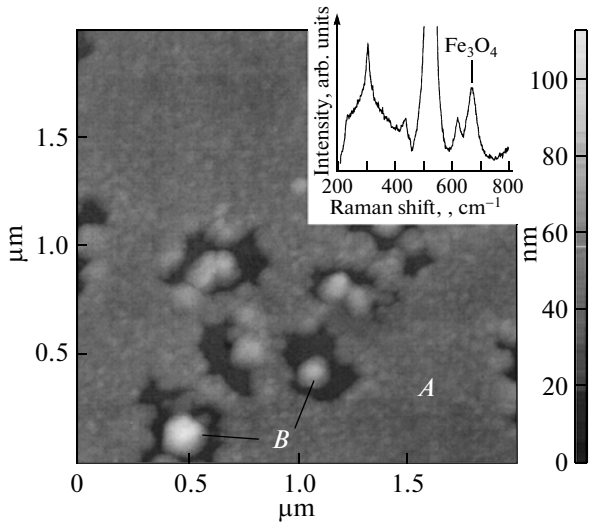

Fig. 2. AFM image taken from the surface of the Fe_3O_4 film obtained by heating the $Fe_3O_4/SiO_2/Si(111)$ system to 300°C and exposure to the oxygen atmosphere. The inset shows the Raman spectrum for this surface.

In the next experiment, the Fe film was oxidized in the oxygen atmosphere in the course of heating from room temperature to 300°C. At a temperature of about 150°C, diffraction rings from Fe in the RHEED pattern changed to rings from magnetite (Fig. 3a). Such an RHEED pattern was observed both under heating of the film to 300°C and after its subsequent exposure to the oxygen atmosphere at this temperature for 10 min. The RHEED pattern from the iron oxide film thus grown exhibits rings with a nonuniform distribution of the intensity. This indicates the presence of texture or, in other words, a preferential orientation of crystallites along some direction. The texture in the magnetite film was analyzed by calculating the theoretical RHEED pattern using the kinematic approach [12, 18]. It was found that the magnetite film has [100] texture the axis of which is normal to the surface of the film. The calculated pattern for this texture is shown in Fig. 3b. Since for this texture the [100] direction in the crystallite lattice is oriented largely normally to the plane of the film, the (100) diffraction spot/reflection will be largely located on the normal unlike reflections of other orders. Measurements of angular broadening $\Delta\varphi$ of the (100) reflection show that the [100] axis of the crystallite lattice is offset from the normal to the surface within ±20°.

The presence of [100] texture in the magnetite film can be related to the specific oxidation of the Fe film with [110] texture starting from low temperatures. It was found [19] that the oxidation of an epitaxial Fe film (on a GaAs substrate) leads to the formation of a

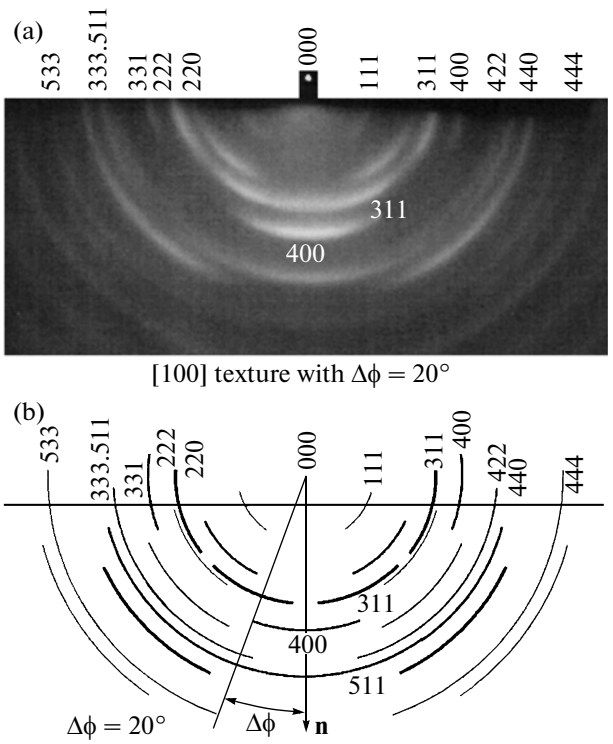

Fig. 3. (a) RHEED pattern obtained upon heating the Fe layer to 300°C in the oxygen atmosphere and (b) the calculated transmission diffraction pattern for the polycrystalline Fe_3O_4 film with [100] texture.

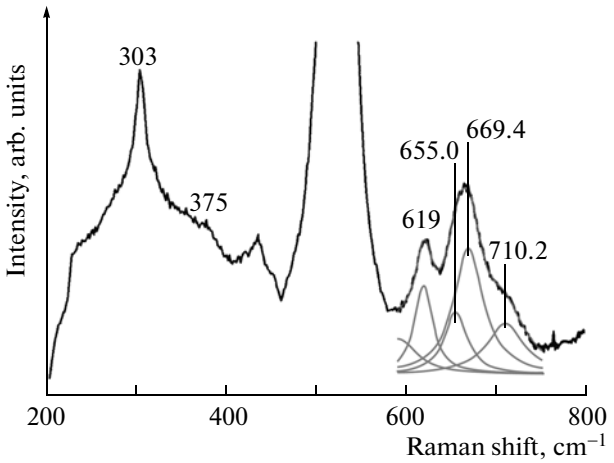

Fig. 4. Raman spectrum for the Fe_3O_4 film obtained by heating the Fe layer deposited at room temperature to 300°C in the oxygen atmosphere. The magnetite peak at 669 cm^{-1} is decomposed into a set of Gaussian curves.

magnetite film with a crystal lattice rotated through 45° relative to the Fe lattice (this rotation is consistent with the angle between the $[110]^{Fe}$ and $[100]^{Fe_3O_4}$ directions in the cubic lattice). The growth of a magnetite film with a preferred orientation was also observed in experiments on magnetron sputtering of iron in an oxygen atmosphere on both the pure and oxidized silicon surface [21]. Interestingly, such an orientation arises when the oxygen pressure (flow rate) is low. Presumably, under these conditions, first Fe crystallites with the [110] orientation originate and then, at subsequent growth stages, they oxidize to form a Fe_3O_4 film with the [100] orientation.

The AFM image shows that the morphology of the film is uniform with an island mean size of ~40 nm. However, the Raman spectrum (Fig. 4) contains not only the magnetite peak at 669 cm^{-1} but also peaks of another phase. The decomposition of the magnetite peak into Gaussian components allowed us to discern peaks at 655 and 710 cm^{-1}. The positions of the peaks, as well as of a "zooming" in the silicon peak at 375 cm^{-1}, are consistent with those of magnetite peaks [22].

When Fe was deposited in the oxygen atmosphere at 300°C, diffraction rings from the polycrystalline magnetite film were observed at the early stage of growth. The RHEED pattern from the iron oxide film thus grown (Fig. 5a) contains diffraction rings typical of textured films. Unlike the previous result (Fig. 3a), here the rings are diffuse and the intensity distribution is different. Analysis showed that the experimental RHEED pattern is best fitted by a theoretical pattern calculated for a film with [311] texture (Fig. 5b) the axis of which is parallel to normal **n** to the film surface. For this structure, the (311) reflection is placed largely on the normal in contrast to reflections of another order. Offset$\Delta\varphi$ of the [311] axis of the crystallite lattice from the normal to the surface is within ±10°. The fact that here the rings are diffuse, unlike for the oxidized Fe film (Figs. 1b, 3b), indicates a small size of crystallites. Indeed, from the AFM image of this surface, it follows that the crystallite mean size is 17 nm, which is almost three times smaller than in the oxidized Fe film. In addition, the AFM image shows that the film has a narrow crystallite size distribution with a density of ~1.1×10^{11} cm^{-2}.

Magnetite films with [311] texture grew also on a SiO_2 amorphous substrate [23] and on the silicon surface covered by a thick (20 nm) [4] and ultrathin (1.5 nm) [7] SiO_2 layer. It follows from experimental data that this texture may arise under magnetron sputtering of Fe in the oxygen atmosphere [23], electron-beam evaporation of a Fe_3O_4 source [4], and laser evaporation of an α-Fe_2O_3 source [7]. We suppose that this texture results from the so-called competitive growth [24] because of a low growth temperature and a low atomic mobility. The decrease in the mobility of Fe atoms or Fe oxide molecules on the growing surface may be associated both with a low growth temperature and with a high deposition rate of the material. In fact, the growth temperature of Fe_3O_4 films in [4, 23] was as low as 20 and 50°C, respectively. Moreover, magnetite films with [311] texture were also grown on a pure Si(100) substrate at room temperature [20]. At the same time, high-temperature deposition (at 400 and

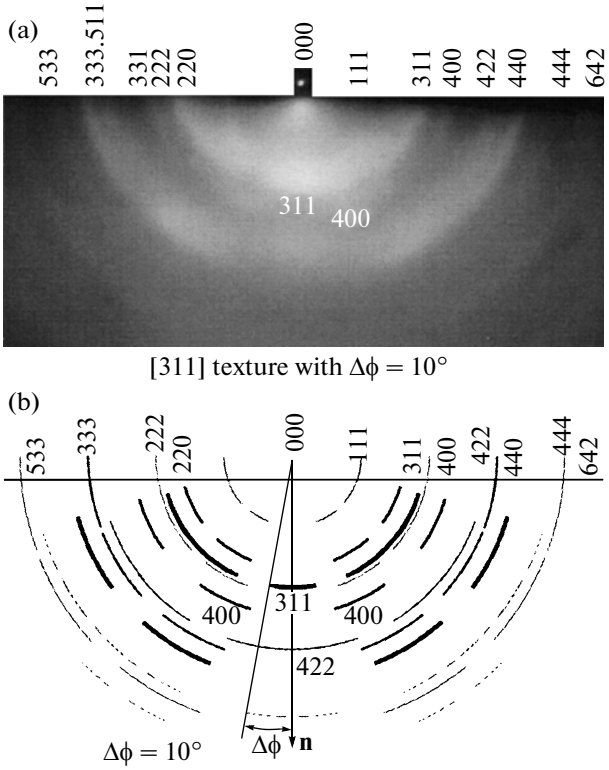

Fig. 5. (a) RHEED pattern obtained upon depositing the Fe layer at 300°C in the oxygen atmosphere and (b) the calculated transmission diffraction pattern for the polycrystalline Fe_3O_4 film with [311] texture.

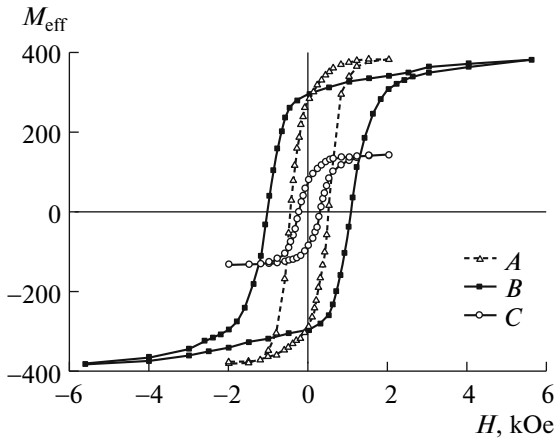

Fig. 6. Hysteresis loops for 16 nm thick Fe_3O_4 films on the surface of the SiO_2/Si(111) structure that were obtained by (*A*) annealing of the Fe layer deposited at room temperature at 300°C in the oxygen atmosphere, (*B*) heating of the Fe layer deposited at room temperature to 300°C in the oxygen atmosphere, and (*C*) deposition of the Fe layer in the oxygen atmosphere at 300°C.

450°C) on different substrates (glass, silicon) results in the growth of magnetite films with [111] texture [3, 5]. Transmission electron microscopy data showed [5] that, in the case of iron magnetron-sputtered in the oxygen atmosphere, the growth of an amorphous iron oxide layer changes to the growth of a polycrystalline Fe_3O_4 film with [111] texture irrespective of the type of silicon substrate (Si(111) or Si(001)). This orientation of Fe_3O_4 films seems to result from the restructuration/coalescence growth [24]. In this case, crystal faces with the lowest free energy are parallel to the substrate surface and the texture axis is parallel to the respective crystal directions. Since the (111) faces of Fe_3O_4 crystals have the lowest free energy [25], the texture axis is expected to be normal to the surface and coincide with the [111] direction. In such a configuration, randomly oriented Fe_3O_4 crystallites grow from an amorphous iron oxide layer and the [111] growth texture results from the preferential lateral growth of those Fe_3O_4 crystallites the (111) surface of which is oriented parallel to the substrate surface. At the same time, the combination of a high Fe and O_2 (+Ar) vapor pressure (1 Pa) with a low growth temperature (20°C) causes the growth of an untextured Fe_3O_4 film with an amorphous phase between crystallites [26].

While iron oxide crystallites and iron silicide crystallites may form simultaneously when a Fe film is deposited in the oxygen atmosphere, the Raman spectroscopy data show the presence of a single-phase magnetite film. Silicidation in the SiO_2 film is limited by the surface diffusion (delivery) of Fe atoms to defects and, correspondingly, by the interdiffusion of Si and Fe atoms through defect sites. We suppose that this process is feeble, whereas the nucleation of iron oxide crystallites as a result of interaction between Fe atoms and O_2 molecules arriving at the surface dominates. The uniformity of the film consisting of equisized (~17 nm) islands and the absence of a signal from iron silicide in the RHEED pattern and in the Raman spectrum confirm the complete oxidation of iron and formation of magnetite.

Figure 6 shows hysteresis loops for the magnetite films obtained by different techniques. Measurements showed that the rotation of the sample about an axis normal to the substrate surface does not influence the shape of hysteresis loops, indicating the absence of magnetic anisotropy. As follows from Fig. 6, the effective magnetization of the Fe_3O_4 film obtained by the oxidation of the Fe film (loops *A* and *B*) is higher than that of the Fe_3O_4 film obtained by iron deposition in the oxygen atmosphere (loop *C*). This is because the grain size in the films corresponding to loops *A* and *B* is more than twice as large as the grain mean size in the film obtained by iron deposition in the oxygen atmosphere. For the same reason, the magnetite films corresponding to loops *A* and *B* have a higher value of the hysteresis loop rectangularity coefficient: M_r/M_s = 0.77 versus ~0.6 for the film corresponding to loop *C*.

According to earlier experimental data on the magnetic properties of epitaxial [9, 27] and polycrystalline [5, 28] magnetite films, coercive force H_c of the films about 100 nm thick roughly equals 300 Oe. In our

experiments, the film obtained by iron deposition in the oxygen atmosphere has a close value of the coercive force, 270 Oe (curve *C*). The magnetite films obtained by oxidation of Fe films have higher values of the coercive force (loops *A* and *B*; $H_c = 505$ and 1000 Oe, respectively). Possible reasons are porosity, coarser grains [29], a larger peak-to-valley height [30], and the presence of interfaces between iron silicide phases (loop *A*) and γ-Fe_2O_3 (loop *B*). For epitaxial films, it was noted [27] that the coercive force of unstrained Fe_3O_4/MgO films is ~280 Oe, while in Fe_3O_4/Sr_3TiO_4 films strained because of a large amount of dislocations, it rises to ~600 Oe. It can be supposed that the nonuniformity of the films in structure and composition increases the coercive force.

CONCLUSIONS

The structural and magnetic properties of Fe_3O_4 films grown on the Si(111) surface covered by a thin SiO_2 layer are investigated. The formation of magnetite films by oxidizing a deposited Fe layer and by depositing a Fe layer on the surface of the SiO_2/Si(111) structure in the oxygen atmosphere is considered. It is found that Fe_3O_4 films obtained by oxidation of a Fe layer in the oxygen atmosphere are nonuniform in structure and phase composition. Magnetite films obtained by high-temperature oxidation of Fe contain iron monosilicide. At the same time, the oxidation of a Fe layer starting from low temperatures results in the formation of the γ-Fe_2O_3 phase. RHEED patterns show that texture in Fe_3O_4 films depends on the film growth method. Fe_3O_4 films obtained by oxidation of Fe has [100] texture, while those obtained by deposition of Fe in the oxygen atmosphere has [311] texture. It is found that the coercive force of magnetite films obtained by oxidation of Fe is two to three times higher than that of films obtained by deposition of Fe in the oxygen atmosphere. A higher value of the coercive force in the former case may be related to a larger grain size, higher surface roughness, and the presence of interfaces between ε-FeSi and γ-Fe_2O_3. At the same time, the coercive force of magnetite films obtained by deposition of Fe in the oxygen atmosphere is comparable to that of Fe_3O_4 films prepared by other methods [5, 28].

ACKNOWLEDGMENTS

The authors thank V.A. Vikulov and E.A. Chusovitin for assistance.

This work was supported by grants from the Far East Branch, Russian Academy of Sciences (grant nos. 09-III-A-02-023 and 09-I-OFN-057) and by the program in support of leading scientific schools (grant no. NSh-46342010.2).

REFERENCES

1. Z. Zhang and S. Satpathy, Phys. Rev. B **44**, 13319 (1991).
2. M. L. Parames, J. Mariano, Z. Viskadourakis, N. Popovici, M. S. Rogalski, J. Giapintzakis, and O. Conde, Appl. Surf. Sci. **252**, 4610 (2006).
3. S. Tiwari, R. Prakash, R. J. Choudhary, and D. M. Phase, J. Phys. D: Appl. Phys. **40**, 4943 (2007).
4. S. Jain, A. O. Adeyeye, and C. B. Boothroyd, J. Appl. Phys. **97**, 093713 (2005).
5. C. Boothman, A. M. Sanchez, and S. van Dijken, J. Appl. Phys. **101**, 123903 (2007).
6. S. Jain, A. O. Adeyeye, and D. Y. Dai, J. Appl. Phys. **95**, 7237 (2004).
7. X. Wang, Y. Sui, J. Tang, C. Wang, X. Zhang, Z. Lu, Z. Liu, W. Su, X. Wei, and R. Yu, Appl. Phys. Lett. **92**, 012122 (2008).
8. T. Taniyama, T. Mori, K. Watanabe, E. Wada, M. Itoh, and H. Yanagihara, J. Appl. Phys. **103**, 07D705 (2008).
9. R. J. Kennedy and P. A. Stamp, J. Phys. D: Appl. Phys. **32**, 16 (1999).
10. A. Ishizaka and Y. Shiraki, J. Electrochem. Soc. **133**, 666 (1986).
11. N. Minami, D. Makino, T. Matsumura, C. Egawa, T. Sato, K. Ota, and S. Ino, Surf. Sci. **514**, 211 (2002).
12. S. Andrieu and P. Frechard, Surf. Sci. **360**, 289 (1996).
13. J. Derrien, J. Chevrier, Vinh Le Thanh, I. Berbezier, C. Giannini, S. Lagomarsino, and M. G. Grimaldi, Appl. Surf. Sci. **73**, 90 (1993).
14. E. J. W. Verwey and E. L. Heilmann, J. Chem. Phys. **15**, 174 (1947).
15. J. L. Verbe, Phys. Rev. B **9**, 5236 (1974).
16. V. V. Balashev, V. V. Korobtsov, T. A. Pisarenko, and E. A. Chusovitin, Fiz. Tverd. Tela (St. Petersburg) **51**, 565 (2009) [Phys. Solid State **51**, 601 (2009)].
17. P. Nyhus, S. L. Cooper, and Z. Fisk, Phys. Rev. B **51**, 15626 (1995).
18. D. Litvinov, T. O'Donnell, and R. Roy, J. Appl. Phys. **85**, 2151 (1999).
19. Y. X. Lu, J. S. Claydon, Y. B. Xu, S. M. Thompson, K. Wilson, and G. van der Laan, Phys. Rev. B **70**, 233304 (2004).
20. Chih-Huang Lai, Po-Hsiang Huang, and Ye-Jen Wang, J. Appl. Phys. **95**, 7222 (2004).
21. G. Zhang, C. Fan, L. Pan, F. Wang, P. Wu, H. Qiu, Y. Gu, and Y. Zhang, J. Magn. Magn. Mater. **293**, 737 (2005).
22. I. Chamritski and G. Burns, J. Phys. Chem. B **109**, 4965 (2005).
23. Y. Kim and M. Oliveria, J. Appl. Phys. **75**, 431 (1994).

24. P. B. Barna and M. Adamik, *Science and Technology of Thin Films*, Ed. by F. C. Matacotta and G. Ottaviani (World Sci., Singapore, 1995), Part 1, pp. 1–29.
25. S. J. Clemett, K. L. Thomas-Keprta, J. Shimmin, M. Morphew, J. R. McIntosh, D. A. Bazylinski, J. L. Kirschvink, S. J. Wentworth, D. S. McKay, H. Vali, E. K. Gibson, Jr., and C. S. Romanek, Am. Mineral. **87**, 1727 (2002).
26. W. B. Mi, Liu Hui, Z. Q. Li, P. Wu, E. Y. Jiang, and H. L. Bai, J. Phys. D: Appl. Phys. **39**, 5109 (2006).
27. Y. Z. Chen, J. R. Sun, Y. N. Han, X. Y. Xie, J. Shen, C. B. Rong, S. L. He, and B. G. Shen, J. Appl. Phys. **103**, 07D703 (2008).
28. J. Tang, K.-Y. Wang, and W. Zhou, J. Appl. Phys. **89**, 7690 (2001).
29. V. I. Malyutin, V. E. Osukhovskii, A. A. Ivanov, L. A. Chebotkevich,I. V. Lobov, and Yu. D. Vorobiev, Phys. Status Solidi A **93**, 585 (1986).
30. S. P. Li, A. Samand, W. S. Lew, Y. B. Xu, and J. A. C. Bland, Phys. Rev. B **61**, 6871 (2000).